Abrupt ice-age shifts in southern westerly winds and Antarctic climate forced from the north

Christo Buizert[1], Michael Sigl[2], Mirko Severi[3], Bradley R. Markle[4], Justin J. Wettstein[1,5], Joseph R. McConnell[6], Joel B. Pedro[7,8], Harald Sodemann[5], Kumiko Goto-Azuma[9], Kenji Kawamura[9], Shuji Fujita[9], Hideaki Motoyama[9], Motohiro Hirabayashi[9], Ryu Uemura[10], Barbara Stenni[11], Frédéric Parrenin[12], Feng He[1,13], T.J. Fudge[4] and Eric J. Steig[4]

[1]College of Earth, Ocean and Atmospheric Sciences, Oregon State University, Corvallis OR 97331, USA

[2]Laboratory of Environmental Chemistry, Paul Scherrer Institute, Villigen, Switzerland

[3]Department of Chemistry "Ugo Schiff", University of Florence, Florence, Italy

[4]Department of Earth and Space Science, University of Washington, Seattle WA 98195, USA [5]Geophysical Institute and Bjerknes Centre for Climate Research, University of Bergen, 5020 Bergen, Norway

[6]Desert Research Institute, Nevada System of Higher Education, Reno, NV 89512, USA

[7]Centre for Ice and Climate, Niels Bohr Institute, University of Copenhagen, Copenhagen, Denmark

[8]Antarctic Climate & Ecosystems Cooperative Research Centre, University of Tasmania, Private Bag 80, Hobart, Tasmania 7001, Australia

[9]National Institute for Polar Research, Tachikawa, Tokyo, Japan

[10]Department of Chemistry, Biology and Marine Science, University of the Ryukyus, Okinawa, Japan

[11]Department of Environmental Sciences, Informatics and Statistics, Ca' Foscari University of Venice, 30172 Venezia, Italy

[12]Université Grenoble Alpes, CNRS, IRD, IGE, 38000 Grenoble, France

[13]Center for Climatic Research, Nelson Institute for Environmental Studies, University of Wisconsin-Madison, Madison WI 53706, USA

The Southern Hemisphere (SH) mid-latitude westerly winds play a central role in the global climate system via Southern Ocean upwelling[1], carbon exchange with the deep ocean[2], Agulhas Leakage[3], and possibly Antarctic ice sheet stability[4]. Meridional shifts of the SH westerlies have been hypothesized in response to abrupt North Atlantic Dansgaard-Oeschger (DO) climatic events of the last ice age[5,6], in parallel with the well-documented shifts of the intertropical convergence zone (ITCZ)[7]. Shifting moisture pathways to West Antarctica[8] are consistent with this view, but may represent a Pacific teleconnection pattern[9]. The full SH atmospheric-circulation response to the DO cycle and its impact on Antarctic temperature remain unclear[10]. Here we use five volcanically-synchronized ice cores to show that the Antarctic temperature response to the DO cycle can be understood as the superposition of two modes: a spatially homogeneous oceanic "bipolar seesaw" mode that lags Northern Hemisphere (NH) climate by about 200 years, and a spatially heterogeneous atmospheric mode that is synchronous with NH abrupt events. Temperature anomalies of the atmospheric mode are similar to those associated with present-day Southern Annular Mode (SAM) variability, rather than the Pacific South America (PSA) pattern. Moreover, deuterium excess records suggest a zonally coherent migration of the SH westerlies over all ocean basins in phase with NH climate. Our work provides a simple conceptual framework for understanding the circum-Antarctic temperature response to abrupt NH climate change. We provide observational evidence for abrupt shifts in the SH westerlies, which has previously-documented[1-3] ramifications for global ocean circulation and atmospheric CO_2. These coupled changes highlight the necessity of a global, rather than a purely North Atlantic, perspective on the DO cycle.

During the glacial DO cycle, abrupt variations in northward heat transport by the Atlantic Meridional Overturning Circulation (AMOC) affect Greenland and Antarctic temperature oppositely (Fig. 1), via an oceanic teleconnection called the bipolar seesaw[6,11]. Antarctica warms during Greenland cold phases (stadials), and cools during Greenland warmth (interstadials), with the gradual nature of Antarctic climate change reflecting buffering by a large heat reservoir[11] – likely the global ocean interior[6]. The DO cycle affects atmospheric circulation also; the ITCZ shifts southwards during stadials, and northwards during interstadials[7]. General Circulation Model (GCM) simulations suggest parallel shifts of the SH westerlies[5,6,12], but the available observational evidence (a deuterium excess record from West Antarctica[8]) cannot distinguish between such shifts and Pacific-only teleconnections[9]. Furthermore, the impact of the atmospheric circulation changes on Antarctic climate remains unknown, and models are inconclusive on this question[10,13].

We use water stable isotope ratios, a proxy for site temperature[14], from five Antarctic ice cores: WAIS (West Antarctic Ice Sheet) Divide (WDC), EPICA (European Project for Ice Coring in Antarctica) Dronning Maud Land (EDML), EPICA Dome C (EDC), Dome Fuji (DF) and Talos Dome (TAL). WDC is synchronized to Greenland ice cores at high precision via atmospheric methane (Fig. 1a, b)[15]; here we synchronize WDC to the other cores in the 10-57 ka before present (BP) interval using volcanic markers (Methods; Extended Data Figure 1), greatly improving our ability to study the timing of regional Antarctic climate variations relative to Greenland. The Antarctic response to DO events is investigated using a stacking technique, in which 19 individual events are aligned at the midpoint of their abrupt methane transition in the WDC core, and averaged to obtain the shared climatic signal (Methods).

Antarctica cools in response to DO warming (Fig. 2a, b), consistent with the bipolar seesaw theory[6,11]. In the Antarctic mean $\delta^{18}O$ stack, the cooling onset occurs about two centuries after the abrupt NH event, providing validation of earlier results from West Antarctica[15]. There is a spatial pattern to the Antarctic response, however. A step-like divergence from the mean signal is seen around $t \approx 0$ yr (i.e., synchronous with NH climate), with the interior East Antarctic Plateau sites (DF and EDC) warming, and EDML cooling (Fig. 2c). This instantaneous warming over the Plateau is particularly pronounced at DO events 1, 8, 12 and 14 (Fig. 1d, red curve).

Using principal component analysis (PCA, see Methods), we find that two modes of variability explain over 96% of signal variance in the five stacked records (Fig. 2d). The first principal component (PC1, 83% of variance explained) has the triangular shape of the Antarctic Isotope Maximum events – the classic thermal bipolar seesaw signal[11] – with a spatially homogeneous expression (Fig. 2f). The two-century lag behind Greenland warming identifies PC1 as an ocean-propagated response[15].

The second principal component (PC2, 13% of variance explained) is a step-like function with a heterogeneous spatial pattern (Fig. 2g). This mode is very different from the bipolar seesaw. The PC2 response is synchronous with NH warming within precision (28 ± 40 year lag); this timing, and additional evidence presented below, suggest this mode represents an atmospheric teleconnection. The PCA does not necessarily separate physical processes. We assume two underlying teleconnections: oceanic (two-century lag) and atmospheric (synchronous). Some amount of each process is included in PC1, as evident by some immediate warming around t=0. We perform a rotation of the PCA vectors (Methods) to isolate the "purely" oceanic and atmospheric responses (Fig. 2e). The associated estimate of the atmospherically-forced

temperature anomaly (Fig. 2h) is cooling at EDML, warming at DF, EDC and TAL, and a negligible response at WDC; this pattern is robustly reproduced using different methods (Extended Data Fig. 6). The magnitude of the Antarctic atmospheric response is roughly proportional to the Greenland ice core $\delta^{18}O$ perturbation (Extended Data Fig. 4).

The Antarctic response to DO cooling is qualitatively similar to the DO warming case. The ocean seesaw warming response is delayed by 226 ± 44 years and the EOF2 spatial pattern has the opposite sign – i.e. additional warming at EDML, and cooling on the interior East Antarctic Plateau (Extended Data Fig. 7). The atmospheric signal over Antarctica is much weaker for the DO cooling case, with PC2 explaining only 9% of variance. This difference is likely due to the fact that DO warmings are more abrupt and of larger magnitude than DO coolings.

To better understand the atmospheric mode, we turn to deuterium excess (*d*), a proxy for vapor source conditions[16] commonly used to identify changes in atmospheric circulation and vapor transport pathways[8,17,18]. In isotope-enabled GCM simulations, Antarctic *d* is anti-correlated with the Southern Annular Mode (SAM) index[8,19]. This anti-correlation can be understood conceptually: when the SH westerlies are displaced equatorward (negative SAM phase), Antarctic moisture will originate further north where sea-surface temperature (SST) is higher and relative humidity lower (Extended Data Fig. 8b), both of which act to make *d* more positive[16]. We use the logarithmic definition of deuterium excess (d_{ln}), which better preserves isotopic moisture source information than the linear definition[8,20].

The Antarctic mean d_{ln} response (Figs. 3a, b) lags NH climate by 8 ± 48 years for DO warming, and 9 ± 42 years for DO cooling, respectively, consistent with previous results for WDC[8]. The observed

d_{ln} response is consistent with a shift in the meridional position of the SH westerly winds and vapor origin, such that they move equatorward in response to NH warming, and poleward in response to NH cooling. The timing suggests propagation to the SH high-latitudes via an atmospheric teleconnection. The d_{ln} response is largest for the interior Plateau sites (DF, EDC), possibly because their vapor source areas are more distant from confounding local effects such as the sea-ice edge[21]. The response is weak or absent at EDML; possibly because SH westerlies' variability is relatively weak in the Atlantic sector (Extended Data Fig. 9), or because of regional effects such as wind-driven changes to the sea ice, gyre circulation or Weddell Sea deep convection[22]. Critically, the four cores that do show a clear d_{ln} response collectively sample water vapor from all ocean basins (Extended Data Fig. 8a), suggesting the changes to the SH atmospheric circulation are zonally coherent and involve all ocean basins (rather than just the Pacific basin as demonstrated previously with WDC).

Figure 4a compares the two independent signals we attribute to a change in atmospheric circulation: PC2 of the $\delta^{18}O$ response, and the Antarctic mean d_{ln} response. Their time evolution is nearly identical, suggesting they are distinct but consistent manifestations of the atmospheric circulation change. The SAM and Pacific-South American (PSA) pattern are the leading modes of large-scale SH atmospheric variability with strong influence on Antarctic temperature[9,23]. We focus our analysis on East Antarctica, where we infer the largest response. The SAM (Fig. 4b) clearly impacts East Antarctic surface air temperature (SAT) strongly (correlation $|r|$ up to 0.65), and with the correct sign to explain the warming seen at EDC, DF and TAL. East Antarctic warming is seen for a more negative SAM index, driven primarily by anomalous atmospheric heat advection[24] (the observed cooling at EDML is discussed below). The PSA (Fig. 4c), on the other

hand, is not meaningfully correlated with SAT at the East Antarctic sites ($|r|$ at or below 0.15). We further create a synthetic index that is the projection of the atmospheric loadings (Fig. 2h) onto the reanalysis SAT anomaly at the core locations (Methods). The patterns in SAT and geopotential height associated with this index (Fig. 4d) closely resemble those of the SAM, with warming in East Antarctica, and roughly annular geopotential height anomalies.

These tests suggest that the SAM is the closest present-day analog to the temperature response we identify in the ice core record, corroborating our independent evidence from the d_{ln} data. While the PSA pattern may have been active during the DO cycle, it does not dominate the Antarctic response.

Our data-based inferences on the timing and sign of changes to the SH westerlies/SAM are consistent with coupled atmosphere-ocean GCM simulations in which AMOC transitions are induced by North Atlantic fresh-water forcing[6,12,25]. Such model simulations show a positive shift in SAM index in response to AMOC shutdown and vice versa (Fig. 3a, b); this shift is synchronous with the applied forcing within uncertainty (Extended Data Table 1). Our observed atmospheric response is more gradual than the model-simulated SAM shift, possibly because of (multi-decadal) data resolution in some cores and the fact that the d_{ln} signal integrates over a large moisture source area extending to 20°S.

Next, we address differences between the ice-core data and the modern-day correlation pattern (Fig. 4b), most notably at EDML. The reanalysis correlation pattern captures the SAT response to monthly internal SAM variability, representing atmospheric heat advection anomalies[24]. The ice cores, on the other hand, record the response to a persistent long-term shift in SAM[13,26], driving

changes in SST, stratification and sea ice extent[22,26]. We speculate that on longer timescales the oceanic influence of the Weddell Sea drives the cooling at EDML, due to e.g. enhanced sea ice cover[22] and stratification, and a weakening of the wind-driven Weddell Gyre. The negligible warming response at WDC is consistent with the relatively weak influence of the SAM in West Antarctic seen in monthly reanalysis (Fig. 4b). Our observations may help constrain the long-term response to a persistent SAM shift, on which GCMs disagree[13].

Last, we want to highlight additional structure in the Antarctic $\delta^{18}O$ stacks that is currently not part of scientific discourse on interhemispheric climate coupling. Most notably, Antarctic warming appears to slow down around t=–400 yr (Fig. 2b), forming a secondary change point that precedes the abrupt DO warming events[27]. Likewise, the rate of Antarctic cooling appears to increase 200 years prior to the abrupt DO cooling events (Extended Data Fig. 7b). These secondary change points are subtler than the ones analyzed in this work, have no apparent corresponding features in Antarctic d_{ln} or Greenland climate, and remain unexplained.

In conclusion, our results show that Antarctica is influenced by NH abrupt climate change on two distinct time scales, representing a slow oceanic and a fast atmospheric teleconnection. In particular, we provide observational evidence for zonally-coherent meridional shifts in the SH westerly winds in phase with Greenland DO events, and its impact on Antarctic temperature. Such shifts have implications for global ocean circulation, Southern Ocean upwelling and productivity, and atmospheric CO_2[1-3]. It is therefore paramount to consider the DO cycle from a global, rather than a purely North Atlantic perspective.

References:

1 Marshall, J. & Speer, K. Closure of the meridional overturning circulation through Southern Ocean upwelling. *Nature Geosci* **5**, 171-180 (2012).

2 Toggweiler, J. R., Russell, J. L. & Carson, S. R. Midlatitude westerlies, atmospheric CO_2, and climate change during the ice ages. *Paleoceanography* **21**, PA2005, doi:10.1029/2005pa001154 (2006).

3 Biastoch, A., Boning, C. W., Schwarzkopf, F. U. & Lutjeharms, J. R. E. Increase in Agulhas leakage due to poleward shift of Southern Hemisphere westerlies. *Nature* **462**, 495-U188, doi:10.1038/nature08519 (2009).

4 Pritchard, H. D. *et al.* Antarctic ice-sheet loss driven by basal melting of ice shelves. *Nature* **484**, 502-505, doi:10.1038/nature10968 (2012).

5 Lee, S. Y., Chiang, J. C., Matsumoto, K. & Tokos, K. S. Southern Ocean wind response to North Atlantic cooling and the rise in atmospheric CO_2: Modeling perspective and paleoceanographic implications. *Paleoceanography* **26** (2011).

6 Pedro, J. B. *et al.* Beyond the bipolar seesaw: Toward a process understanding of interhemispheric coupling. *Quat. Sci. Rev.* **192**, 27-46, doi:10.1016/j.quascirev.2018.05.005 (2018).

7 Schneider, T., Bischoff, T. & Haug, G. H. Migrations and dynamics of the intertropical convergence zone. *Nature* **513**, 45-53 (2014).

8 Markle, B. R. *et al.* Global atmospheric teleconnections during Dansgaard-Oeschger events. *Nature Geosci* **10**, 36-40, doi:10.1038/ngeo2848 (2017).

9 Ding, Q., Steig, E. J., Battisti, D. S. & Kuttel, M. Winter warming in West Antarctica caused by central tropical Pacific warming. *Nature Geosci* **4**, 398-403, doi:10.1038/ngeo1129 (2011).

10 Buiron, D. *et al.* Regional imprints of millennial variability during the MIS 3 period around Antarctica. *Quat. Sci. Rev.* **48**, 99-112, doi:10.1016/j.quascirev.2012.05.023 (2012).

11 Stocker, T. F. & Johnsen, S. J. A minimum thermodynamic model for the bipolar seesaw. *Paleoceanography* **18**, 1087, doi:10.1029/2003pa000920 (2003).

12 Rind, D. *et al.* Effects of glacial meltwater in the GISS coupled atmosphere-ocean model: 2. A bipolar seesaw in Atlantic Deep Water production. *Journal of Geophysical Research: Atmospheres (1984–2012)* **106**, 27355-27365 (2001).

13 Kostov, Y. *et al.* Fast and slow responses of Southern Ocean sea surface temperature to SAM in coupled climate models. *Clim. Dyn.* **48**, 1595-1609, doi:10.1007/s00382-016-3162-z (2017).

14 Jouzel, J. *et al.* Validity of the temperature reconstruction from water isotopes in ice cores. *J. Geophys. Res.* **102**, 26471-26487, doi:10.1029/97jc01283 (1997).

15 WAIS-Divide-Project-Members. Precise interpolar phasing of abrupt climate change during the last ice age. *Nature* **520**, 661-665, doi:10.1038/nature14401 (2015).

16 Merlivat, L. & Jouzel, J. Global climatic interpretation of the deuterium-oxygen 18 relationship for precipitation. *J. Geophys. Res.* **84**, 5029-5033, doi:10.1029/JC084iC08p05029 (1979).

17 Masson-Delmotte, V. *et al.* GRIP Deuterium Excess Reveals Rapid and Orbital-Scale Changes in Greenland Moisture Origin. *Science* **309**, 118-121 (2005).

18 Masson-Delmotte, V. *et al.* Abrupt change of Antarctic moisture origin at the end of Termination II. *Proc. Natl. Acad. Sci. U. S. A.* **107**, 12091-12094, doi:10.1073/pnas.0914536107 (2010).

19 Schmidt, G. A., LeGrande, A. N. & Hoffmann, G. Water isotope expressions of intrinsic and forced variability in a coupled ocean-atmosphere model. *J. Geophys. Res.* **112** (2007).

20 Uemura, R. *et al.* Ranges of moisture-source temperature estimated from Antarctic ice cores stable isotope records over glacial–interglacial cycles. *Clim. Past* **8**, 1109-1125, doi:10.5194/cp-8-1109-2012 (2012).

21 Sodemann, H. & Stohl, A. Asymmetries in the moisture origin of Antarctic precipitation. *Geophys. Res. Lett.* **36**, L22803, doi:10.1029/2009gl040242 (2009).
22 Lefebvre, W., Goosse, H., Timmermann, R. & Fichefet, T. Influence of the Southern Annular Mode on the sea ice–ocean system. *J. Geophys. Res.* **109**, C09005, doi:10.1029/2004JC002403 (2004).
23 Thompson, D. W. J. & Wallace, J. M. Annular Modes in the Extratropical Circulation. Part I: Month-to-Month Variability*. *J. Clim.* **13**, 1000-1016, doi:10.1175/1520-0442(2000)013<1000:amitec>2.0.co;2 (2000).
24 Sen Gupta, A. & England, M. H. Coupled ocean-atmosphere-ice response to variations in the Southern Annular Mode. *J. Clim.* **19**, 4457-4486 (2006).
25 Liu, Z. *et al.* Transient Simulation of Last Deglaciation with a New Mechanism for Bolling-Allerod Warming. *Science* **325**, 310-314, doi:10.1126/science.1171041 (2009).
26 Ferreira, D., Marshall, J., Bitz, C. M., Solomon, S. & Plumb, A. Antarctic Ocean and Sea Ice Response to Ozone Depletion: A Two-Time-Scale Problem. *J. Clim.* **28**, 1206-1226, doi:10.1175/JCLI-D-14-00313.1 (2014).
27 Raisbeck, G. M. *et al.* An improved north–south synchronization of ice core records around the 41 kyr 10Be peak. *Clim. Past* **13**, 217-229, doi:10.5194/cp-13-217-2017 (2017).
28 Grootes, P. M., Stuiver, M., White, J. W. C., Johnsen, S. & Jouzel, J. Comparison of oxygen isotope records from the GISP2 and GRIP Greenland ice cores. *Nature* **366**, 552-554 (1993).
29 Rhodes, R. H. *et al.* Enhanced tropical methane production in response to iceberg discharge in the North Atlantic. *Science* **348**, 1016-1019, doi:10.1126/science.1262005 (2015).
30 Dee, D. P. *et al.* The ERA-Interim reanalysis: configuration and performance of the data assimilation system. *Quarterly Journal of the Royal Meteorological Society* **137**, 553-597, doi:10.1002/qj.828 (2011).

Acknowledgements. This work is funded through the U.S. National Science Foundation, grants ANT-1643394 (to C.B. and J.J.W.), ANT-1643355 (to T.J.F. and E.J.S), AGS-1502990 (to F.H.); the Swiss National Science Foundation grant 200021_143436 (to H.S.); CNRS/INSU/LEFE projects IceChrono and CO2Role (to F.P.); JSPS KAKENHI grants 15H01731 (to K.G.-A., H.M. and M.H.), 15KK0027 (to K.K.) and 26241011 (to K.K., S.F. and H.M.); MEXT KAKENHI grant 17H06320 (to K.K., H.M. and R.U.); European Research Council under the European Community's Seventh Framework Programme (FP7/2007–2013)/ERC grant agreement 610055 (to J.B.P.) ; and the NOAA Climate and Global Change Postdoctoral Fellowship program, administered by the University Corporation for Atmospheric Research (F.H.). We acknowledge high-performance computing support from Yellowstone (ark:/85065/d7wd3xhc) provided by NCAR's

Computational and Information Systems Laboratory, sponsored by the NSF. This research used resources of the Oak Ridge Leadership Computing Facility at the Oak Ridge National Laboratory, which is supported by the Office of Science of the U.S. Department of Energy under Contract № DE-AC05-00OR22725. This is TALDICE publication № 52.

Author Contributions. Data analysis by C.B., M.Se., M.Si. and J.J.W.; manuscript preparation by C.B.; volcanic ice core synchronization by M.Si, M.Se., C.B., J.R.M., F.P., S.F. and T.J.F.; GCM simulations and interpretation by F.H., J.B.P. and J.J.W.; Moisture tagging/tracing experiments by B.R.M. and H.S.; Ice core water isotope analysis by K.G-A, K.K., H.M., M.H., R.U., B.S. and E.J.S.; all authors discussed the results and contributed towards improving the final manuscript.

Author Information. Reprints and permissions information is available at www.nature.com/reprints. The authors declare no competing financial interests. Correspondence and requests for materials should be addressed to Christo Buizert (buizertc@oregonstate.edu).

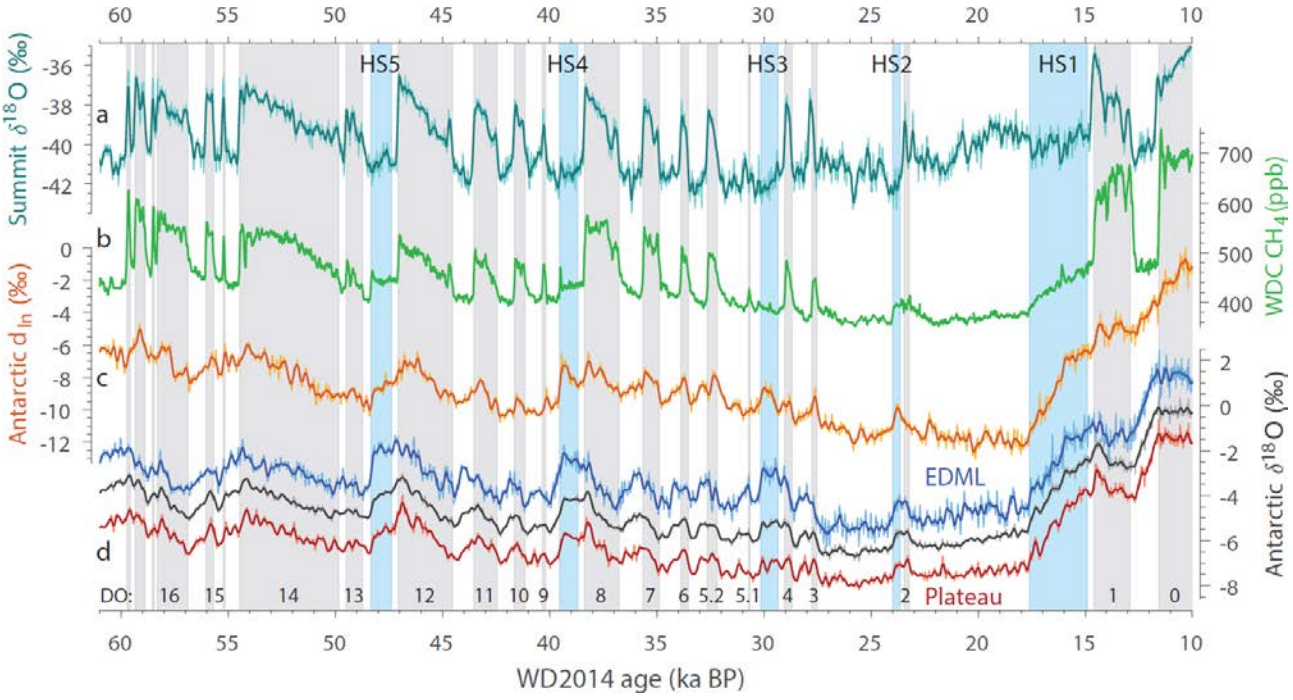

Figure 1 | Records of abrupt glacial climate variability. a, Greenland Summit (average of GISP2 and GRIP[28]) ice core $\delta^{18}O$. **b**, WDC methane[29]. **c**, Antarctic 5-core average d_{ln} anomaly. **d**, Antarctic $\delta^{18}O$ anomaly at EDML (blue), the Antarctic Plateau (average of DF and EDC, red) and 5-core average (black); offset for clarity. All records are synchronized to the WAIS Divide WD2014 chronology; Antarctic data are shown as anomalies relative to present. DO interstadial periods marked in grey and numbered; Heinrich stadials marked in blue. Isotope ratios are on the VSMOW (Vienna Standard Mean Ocean Water) scale. Thin curves show records at original resolution (ranging from ~5 to ~50 years), with the thick lines a moving average (300 and 150 year window for Antarctic and Greenland data, respectively).

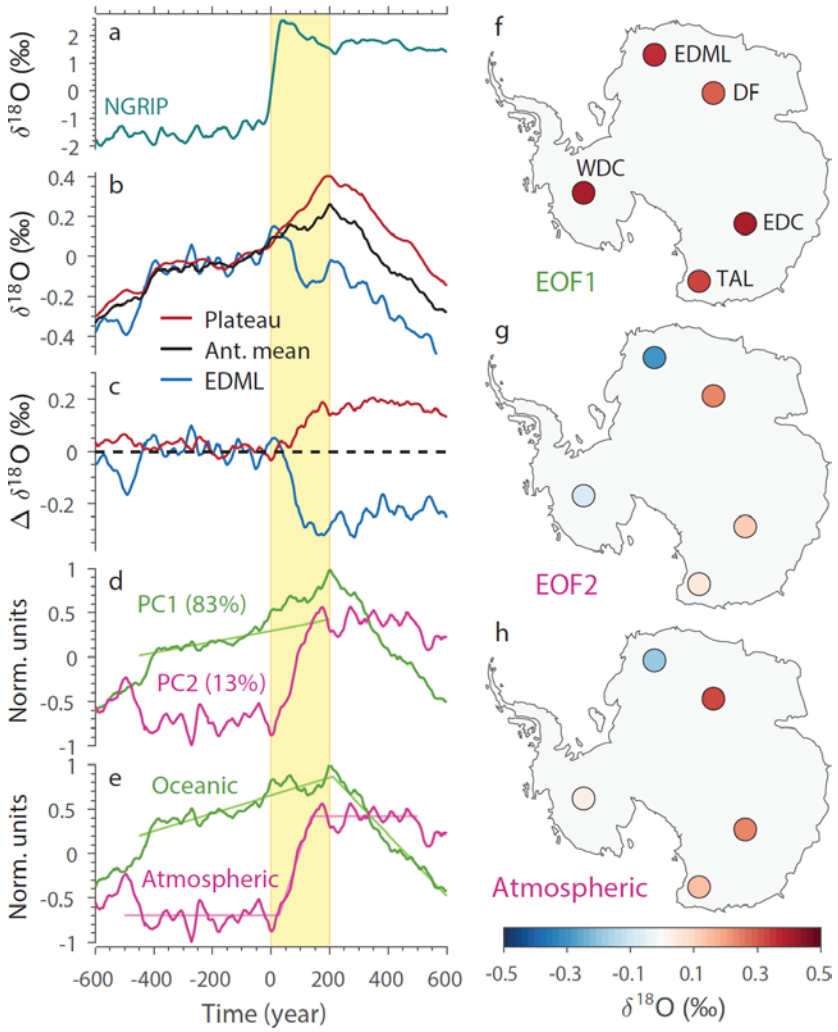

Figure 2 | The Antarctic climate response to DO warming. a, Stack of NGRIP $\delta^{18}O$. **b**, Stack of Antarctic $\delta^{18}O$ at indicated locations, with "Plateau" the average of DF and EDC. **c**, As in **b**, but with 5-core mean subtracted. **d**, First two principal components of the Antarctic $\delta^{18}O$ stacks (1500 yr window), with percentage of variance explained (offset for clarity). PC1 is strongly correlated (r = 0.998) to the Antarctic mean. Linear fit to PC1 (t = -400 to t=0 interval) is shown to highlight the response around t = 0. **e**, Rotated PC1 and PC2 vectors representing proposed oceanic and atmospheric modes, with fits from change point analysis (Methods). The oceanic mode lags by 211 ± 42 years; the atmospheric mode by 28 ± 40 years (1σ bounds; Extended Data Table 1). **f-g**, Empirical Orthogonal Functions EOF1 and EOF2 associated with PC1 and PC2 in **d**, scaled to show the magnitude in permil. **h**, Spatial pattern associated with the atmospheric mode as shown in **e**, scaled to permil. Isotope ratios are on the VSMOW scale.

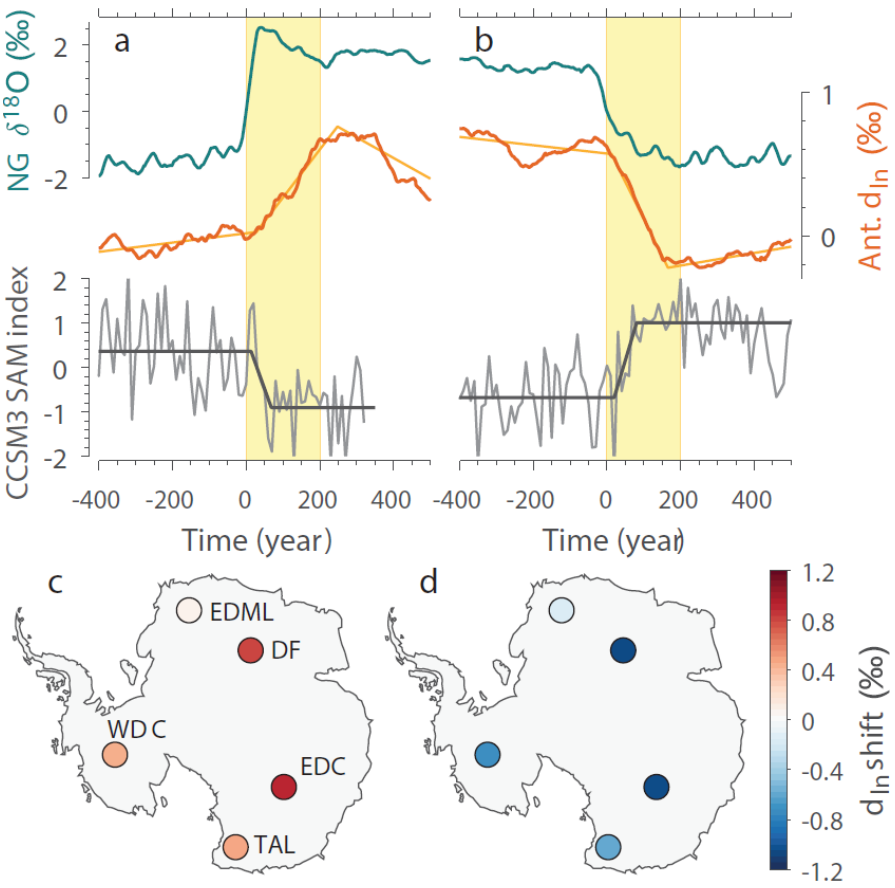

Figure 3| Deuterium excess and the SH westerlies. a, DO warming: Greenland $\delta^{18}O$ stack (turquoise); 5-core average Antarctic d_{ln} stack (orange with BREAKFIT result, see Extended Data Table 1); SAM index (here the leading principal component of sea level pressure variability south of 20°S) following a freshwater-forced AMOC perturbation in CCSM3 (Community Climate System Model version 3) model simulations (grey with fit from change-point analysis, see Extended Data Table 1). **b**, as **a**, but for DO cooling. **c**, Magnitude of Antarctic d_{ln} response to DO warming in permil. The weak d_{ln} trend before and after the abrupt jump likely reflects the SST of SH vapor source waters following the thermal bipolar seesaw[8,11]. **d**, as **c**, but for DO cooling. Isotope ratios are on the VSMOW scale.

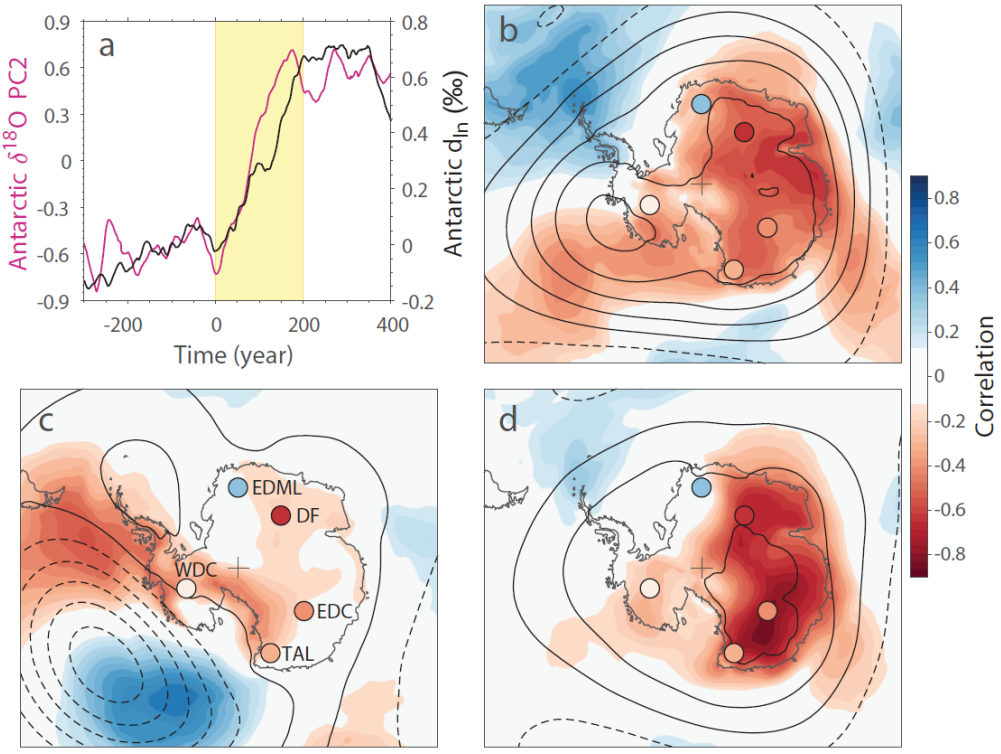

Figure 4 | Attribution of the atmospheric mode of Antarctic temperature variability. a, Comparison of PC2 of the 5 Antarctic $\delta^{18}O$ stacks as in Fig. 2d (pink, left axis) and the Antarctic mean d_{ln} stack as in Fig. 3a (black, right axis). Isotope ratios are on the VSMOW scale. **b**, Correlation between a standardized monthly SAM index and SAT (2-meter temperature) in ERA-Interim[30] for 1979-2017 (shading, scale bar on right) with superimposed 850 hPa geopotential height regressions (10 m contours) and the ice core atmospheric temperature mode from Fig. 2h (circles, scale bar from Fig. 2). Note that regions of anti-correlation are colored red (i.e. warming in response to negative SAM shift). **c**, as panel **b**, but for a standardized PSA index. The SAM and PSA are here taken to be PC1 and PC2 of the 850 hPa geopotential height field south of 20°S, respectively. **d**, as panel **b**, but for a synthetic index of the atmospheric mode created by regressing ERA-Interim SAT anomalies at the ice core sites onto the coefficients in Fig. 2h (Methods).